

Supporting information for

## **Electrochemical CO<sub>2</sub> Reduction in Acidic Electrolytes: Spectroscopic Evidence for Local pH Gradients**

Madeline H. Hicks<sup>1,3,‡</sup> Weixuan Nie<sup>1,3,‡</sup> Annette E. Boehme<sup>2,3</sup>, Harry A. Atwater<sup>\*2,3</sup>, Theodor Agapie<sup>\*1,3</sup> and Jonas C. Peters<sup>\*1,3</sup>

<sup>1</sup> Division of Chemistry and Chemical Engineering, California Institute of Technology, Pasadena, CA, 91125, USA

<sup>2</sup> Department of Applied Physics and Material Science, California Institute of Technology, Pasadena, CA, 91125, USA

<sup>3</sup> Liquid Sunlight Alliance (LiSA), California Institute of Technology, Pasadena, CA, 91125, USA

## Experimental Procedures

### Materials and General Methods

All solvents and reagents were purchased from commercial sources and used as received, unless otherwise noted. Cu and Ag foils (99.999%, 25 mm × 25 mm × 0.5 mm) were purchased from Sigma Aldrich. GDE Cu/PTFE was prepared by sputtering Cu onto the PTFE substrate using the pure Cu metal target (>99.99%) to make a 300 nm layer of Cu particles on PTFE in a sputtering system (AJA INTERNATIONAL INC) under high vacuum condition (5 mTorr). The leakless Ag/AgCl reference electrode was purchased from Innovative Instruments. Platinum foil (99.99% Pt, 25 mm × 25 mm × 0.05 mm) was purchased from Alfa Aesar. Carbon rods (99.999% C) were purchased from Strem Chemicals. A Selemion AMV anion-exchange membrane was purchased from AGC Engineering Co. Phosphoric acid (85 wt.% in H<sub>2</sub>O, 99.99% trace metals basis), potassium chloride (99.999% trace metals basis), lithium chloride (≥99.98% trace metals basis), cesium chloride (≥99.999% trace metals basis), potassium hydroxide (semiconductor grade, pellets, 99.99% trace metals basis (Purity excludes sodium content.)), tetrabutylammonium chloride (≥97.0%, then recrystallized), 18-crown-6 (≥99.0%) and 6,8-dihydroxypyrene-1,3-disulfonic acid disodium salt (DHPDS, ≥97%) were purchased from Sigma Aldrich. Natural abundance CO<sub>2</sub> (Research grade) and Argon (ultra-high purity) were purchased from Airgas. Water was purified by a Nanopure Analytical Ultrapure Water System (Thermo Scientific) or a Milli-Q Advantage A10 Water Purification System (Millipore) with specific resistance of 18.2 MΩ·cm at 25 °C. N-tolyl pyridinium triflate was prepared as reported.<sup>1</sup>

Before each electrochemical experiment, Cu foil was mechanically polished to a mirror-like finish using nanodiamond suspension (3 μm followed by 0.1 μm, Buehler), then rinsed with ultra-pure water and dried under a stream of nitrogen gas. The Cu foil was then electropolished using the following method: +2.3 V vs. a carbon rod electrode was applied to the Cu foil in a phosphoric acid bath (85 wt.%) for 5 minutes and the Cu foil was subsequently washed with copious amounts of ultra-pure water and dried under a stream of nitrogen gas. Platinum foil as the counter electrode was rinsed with ultra-pure water and flame-annealed using a butane torch for 10 s. Nearly-M<sup>+</sup>-free pH = 2 electrolyte (H<sub>3</sub>PO<sub>4</sub>) was prepared by making 0.01 M H<sub>3</sub>PO<sub>4</sub> (85 wt.% in H<sub>2</sub>O, 99.99% trace metals basis) aqueous solution first, with pH then adjusted to ~2.0 using concentrated H<sub>3</sub>PO<sub>4</sub>. Inductively coupled plasma mass spectrometry (ICP-MS) was applied to test the nearly-M<sup>+</sup>-free pH = 2 electrolyte (H<sub>3</sub>PO<sub>4</sub>), showing ~1 ppm M<sup>+</sup> in the solution. pH 2 electrolytes with 0.2 ~ 500 mM M<sup>+</sup> were prepared by adding certain amounts of MCl into nearly-M<sup>+</sup>-free pH = 2 electrolyte (H<sub>3</sub>PO<sub>4</sub>) to make the final [M<sup>+</sup>] as desired. Nearly-M<sup>+</sup>-free pH = 1 electrolyte (H<sub>3</sub>PO<sub>4</sub>) was prepared by making 0.1 M H<sub>3</sub>PO<sub>4</sub> (85 wt.% in H<sub>2</sub>O, 99.99% trace metals basis) aqueous solution first, with pH then adjusted to ~1.0 using concentrated H<sub>3</sub>PO<sub>4</sub>. pH 1 electrolyte with 0.1 M K<sup>+</sup> was prepared by adding 0.1 M [KCl] into the nearly-M<sup>+</sup>-free pH = 1 electrolyte (H<sub>3</sub>PO<sub>4</sub>). Prior to each electrolysis for CO<sub>2</sub> reduction, the electrolyte solutions were

sparged with CO<sub>2</sub> gas for at least 30 min. The pH of electrolytes were measured by a SB90M5 Benchtop symphony Meter with a Mettler Toledo InLab®Routine pH electrode.

## Electrochemical Experiments

Controlled-current electrolysis experiments were carried out in a custom-made PEEK cell setup similar to the one reported by Ager et al.<sup>2</sup> with a copper foil as the working electrode and a platinum foil as the counter electrode. The cathode and anode compartments were separated with a Selemion AMV anion-exchange membrane. Chronopotentiometry (CP) measurements were conducted using a Biologic VMP3 multichannel potentiostat, the working current was set constant and the electrode potential versus a leakless Ag/AgCl reference electrode was measured. The reference electrode was calibrated against a saturated calomel electrode (SCE) (+0.241 V saturated vs. standard hydrogen electrode). Potentiostatic electrochemical impedance spectroscopy (PEIS) measurements were conducted at frequencies ranging from 100 Hz to 200 KHz before each electrolysis experiment to determine the Ohmic resistance of the cell setup. A linear fit was performed in the high-frequency part of the Nyquist plot. The axis intersection was identified as the Ohmic resistance of the cell. The potentiostat was not set for any *iR* drop compensation. The reported electrode *E* was compensated after measurements based on applied current and measured Ohmic resistance of the cell setup.

All experiments were performed at room temperature for 35 min at 25 °C in corresponding electrolytes under CO<sub>2</sub> or Ar atmosphere. The effluent gas stream through the cell (5 mL/min) was flowed into the sample loops of a gas chromatograph (GC-FID/TCD, SRI 8610C, in Multi Gas 5 configuration) equipped with a HayeSep D column. Carbon monoxide, methane and ethylene were detected by a methanizer-flame ionization detector (FID) and hydrogen was detected by a thermal conductivity detector (TCD). Every 10 minutes, 1 mL of gas was sampled to determine the concentration of gaseous products. After electrolysis, the main liquid products (formate, ethanol and 1-propanol) in catholytes were quantified by HPLC (Thermo Scientific Ultimate 3000). For electrolysis with modified Cu/film electrodes, film deposition was first conducted in nearly-M<sup>+</sup>-free pH = 2 electrolyte (H<sub>3</sub>PO<sub>4</sub>) with 15 mM N-tolyl pyridinium triflate under CO<sub>2</sub> on Cu electrodes at -1.25 mA/cm<sup>2</sup> for 35 min. After that, the catholyte and anolyte chambers were rinsed with fresh nearly-M<sup>+</sup>-free pH = 2 electrolyte (H<sub>3</sub>PO<sub>4</sub>) twice before the catholyte and anolyte were refilled with testing electrolytes. The controlled-current electrolysis was conducted using the same method as for bare Cu electrodes.

Electrolysis experiments on GDE Cu/PTFE were conducted in a custom-made flow cell which is composed of a gas flow chamber, a catholyte chamber and an anolyte chamber. Cu/PTFE GDE was clamped between the gas flow chamber and the catholyte chamber with a gasket, with 1 cm × 1 cm Cu catalyst facing the catholyte chamber and PTFE substrate facing the gas flow chamber. 5 standard cubic centimeters per minute (sccm) CO<sub>2</sub> gas flow was applied through the gas flow chamber. A Selemion AMV anion-exchange membrane (AGC Engineering Co.) was used

to separate the catholyte chamber and the anolyte chamber. A piece of Pt mesh was employed as the counter electrode in the anolyte chamber. A leakless Ag/AgCl reference electrode was placed near the Cu catalyst in the catholyte chamber. Electrochemical measurements and chronopotentiometry (CP) were conducted using a Biologic VMP3 multichannel potentiostat. The catholyte and anolyte were pumped through two separate silicon tubes by a peristaltic pump at a constant flow rate of approximately 12.3 mL/min. The electrolytes entered each chamber from the bottom and exited from the top, then flowed back to the bulk electrolyte forming a closed cycle. The pH value of the catholyte was tested before and after electrolysis to confirm the acidic pH of the catholyte during the measurement process. Potentiostatic electrochemical impedance spectroscopy (PEIS) measurements were conducted at frequencies ranging from 100 Hz to 200 KHz before each electrolysis experiment to determine the Ohmic resistance of the flow cell setup using the same method above for the H-cell setup with Cu foils.

The pre-deposition of the additive film on GDE Cu/PTFE was conducted in pH = 2 electrolyte (H<sub>3</sub>PO<sub>4</sub>) containing 15 mM N-tolyl pyridinium triflate (tolyl-pyr) with 5 sccm CO<sub>2</sub> flow. After the electrodeposition, the catholyte and the anolyte were rinsed and changed to testing electrolytes. Additional 1.5 mM tolyl-pyr was added in the catholyte for dynamic film formation on Cu.<sup>3</sup> Chronopotentiometry (CP) at a constant current density of -50 mA/cm<sup>2</sup> was applied on GDE Cu/film with 5 sccm CO<sub>2</sub> flowing through the gas flow chamber behind the PTFE substrate. During the CO<sub>2</sub>R process, the gas stream was flowed into the sample loops of GC-FID/TCD (SRI 8610C, in Multi Gas 5 configuration) to measure the concentration of gas products (H<sub>2</sub>, CO, CH<sub>4</sub> and C<sub>2</sub>H<sub>4</sub>) every 10 min. After electrolysis, the pH of the catholyte was tested and the main liquid products (formic acid, acetic acid, ethanol and 1-propanol) in the catholyte were quantified by HPLC (Thermo Scientific Ultimate 3000).

### **ATR-SEIRAS measurements**

Polycrystalline gold films were chemically deposited (electroless deposition) onto the reflecting plane of a 60° Si prism. The Au thin films were prepared by a chemical plating technique previously reported by Osawa, with slight modifications.<sup>4</sup> The prism was first polished with a 3 μm Al<sub>2</sub>O<sub>3</sub> slurry using 30 “figure 8” motions to polish. The prism was thoroughly rinsed with water, and then the prism was polished with 0.5 μm Al<sub>2</sub>O<sub>3</sub> slurry using 20 “X type” motions to polish. To remove the Al<sub>2</sub>O<sub>3</sub> residue, the prism was sonicated in 50% EtOH/50% H<sub>2</sub>O for 15 minutes and then sonicated in water for 15 minutes. Following cleaning, the reflecting plane of the prism was immersed in NH<sub>4</sub>F for 90 s to remove the oxide layer and create a hydrogen-terminated surface to improve adhesion of the Au film. The Si surface was then immersed in a mixture of the Au plating solution (10 mM NaAuCl<sub>4</sub>·2H<sub>2</sub>O + 0.033 M NH<sub>4</sub>Cl + 0.1 M Na<sub>2</sub>SO<sub>3</sub> + 0.033 M Na<sub>2</sub>S<sub>2</sub>O<sub>3</sub>·5H<sub>2</sub>O) and a 2 wt% hydrofluoric acid solution (in a 2:1 ratio) for 1.5 min at 50 °C. The film quality was checked using a multimeter, where the ideal resistance across the film was between 5-15 Ohms.

For *in situ* ATR-SEIRAS experiments, a Nicolet 6700 FTIR (Thermo Fisher Scientific) with a VeeMax III (PIKE Technologies) ATR configuration chamber was used. A spectral resolution of 4 cm<sup>-1</sup> was used for data collection. Experiments were performed using a custom spectroelectrochemical cell fabricated from PEEK. Following cell assembly, the Au film was covered in 0.1 M H<sub>2</sub>SO<sub>4</sub>, which was deaerated with Ar, and subjected to pretreatment cleaning CV cycles between 0.2 and 1.75 V vs RHE for 20 cycles at 50 mV/s. The electrolyte was removed, and the film was rinsed with water 3 times. Next, 5.75 mM CuSO<sub>4</sub>·5H<sub>2</sub>O in 0.1 M H<sub>2</sub>SO<sub>4</sub> was added to the cell. A copper film was then electrochemically deposited on Au by applying -0.2 V vs Ag/AgCl until a total charge of 100 mC had passed. The electrolyte was removed, and the cell was again rinsed with water. The Cu film was then used as the working electrode for ATR-SEIRAS measurements. With the electrolyte of interest added to the cell, the Cu surface was reduced at -0.2 V vs Ag/AgCl. Following Cu reduction, a background spectrum of 64 scans at 0 V vs RHE was collected. Time-dependent and potential-dependent sample spectra were collected using an average of 20 scans.

### Fluorescence confocal laser scanning microscopy (CLSM) measurements

CLSM measurements were performed with a Leica Stellaris 5 upright confocal microscope with a HC FLUOTAR L 25x/0,95 W VISIR water immersion objective. A custom-made electrochemical cell was 3D-printed. It exhibits a horizontal orientation to be compatible with confocal microscopy. It consists of a flat base plate, topped with a rubber gasket to prevent leakage as well as an electrolyte chamber. A polished copper foil cathode is placed between the gasket and the electrolyte chamber which exhibits a circular hole in the center with an area of 0.2 cm<sup>2</sup> that exposes the copper cathode. The electrolyte chamber is open at the top to allow the water immersion objective to be dipped into the electrolyte. It further has an inlet with a straw that leads to the cathode surface as well as an outlet at the opposite side of the chamber that allows for electrolyte recirculation. A third inlet port enables constantly bubbling the electrolyte with 5 sccm CO<sub>2</sub>. A leakless Ag/AgCl reference electrode and a Pt mesh counter electrode are immersed into the electrolyte (**Figure S16**). pH imaging is possible by the addition of the pH-sensitive dye 6,8-dihydroxypyrene-1,3-disulfonic acid disodium salt (DHPDS) that is sensitive to pH values between 6 and 11.5. Hence, only local pH values exceeding 6 can be resolved. 50 μM DHPDS were dissolved in the electrolyte. The dye molecules were excited separately with a laser beam at 405 nm (laser power 1.2%) and a second laser beam at 448 nm (laser power 0.5%). The emission was collected separately for both excitations between 495 and 835 nm with a gain of 100. The pinhole was set to 1 Airy unit. The ratio between the emission from both excitations is a measure for the local pH value. A calibration curve was determined previously by measuring the ratio of emission for various solutions of known pH value and determining a sigmoidal fit curve (**Figure 1d**). It was determined as

$$pH = 8.153 - \frac{1}{1.651} \ln \left( \frac{10}{(\text{Ratio of Emission}) - 0.01305} - 1 \right).$$

Before each pH imaging experiment, potentiometric electrochemical impedance spectroscopy (PEIS) was performed using a Biologic SP-200 potentiostat. Three-dimensional confocal microscopy images were captured as a time series approximately every 5 seconds. The image format was chosen to be 512 x 16 pixels in the x-y plane with a pixel size of  $\sim 500 \text{ nm} \times 500 \text{ nm}$ . A stack of images in the z-direction (perpendicular to the cathode surface) was captured with a distance of 565 nm, starting at the surface of the cathode to  $\sim 20 \text{ }\mu\text{m}$  above the surface. The local pH value was averaged over all pixels between what was determined to be the cathode surface and  $\sim 1 \text{ }\mu\text{m}$  above the surface as a function of time. The pH maps in **Figure 2c** and **Figure S13** are pH maps in the x-z plane, averaged over the 16 pixels in the y direction. A constant current of  $\langle j \rangle = -1.25 \text{ mA/cm}^2$ ,  $-5.00 \text{ mA/cm}^2$  or  $-10.0 \text{ mA/cm}^2$  was applied 30 seconds after starting a confocal time series. Fresh electrolyte with unused DHPDS dye was used for each time series measurement and the cell and objective were rinsed extensively with nanopure water between each experiment. The electrolyte was circulated through the cell at a rate of 1 mL/min during measurements to mitigate the buildup of bubbles that impede pH imaging. Large bubbles still formed at high current densities. In that case, the measurement was interrupted, the bubbles were removed with a glass pipette and the measurement was resumed. This caused gaps and noise in the data obtained at higher current densities, however, the pH trend is still clearly distinguishable. During the course of a measurement, the buildup of bubbles intensified which is why the duration of CLSM confocal measurements was limited to 10 minutes.

## Supporting Figures and Tables

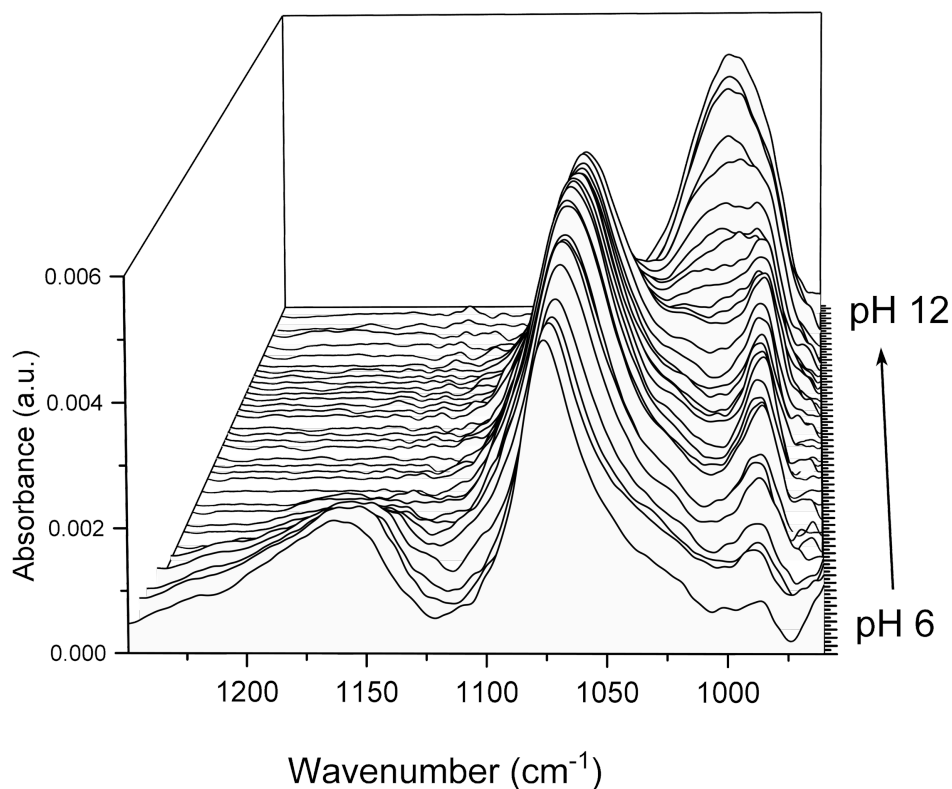


**Figure S1.** ATR-SEIRAS phosphate calibration spectra recorded between pH 6-13 by the addition of KOH to the initial KH<sub>2</sub>PO<sub>4</sub> solution and recording a spectrum every ~0.4 pH units at a constant potential of 0 V<sub>RHE</sub>

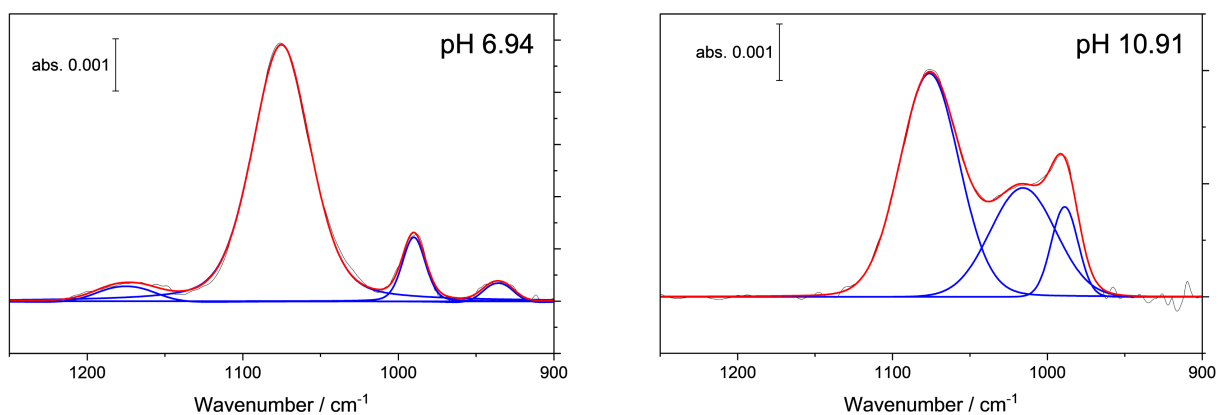


**Figure S2.** Peak deconvolution for phosphate region for pH determination. Peaks were deconvoluted using Matlab.

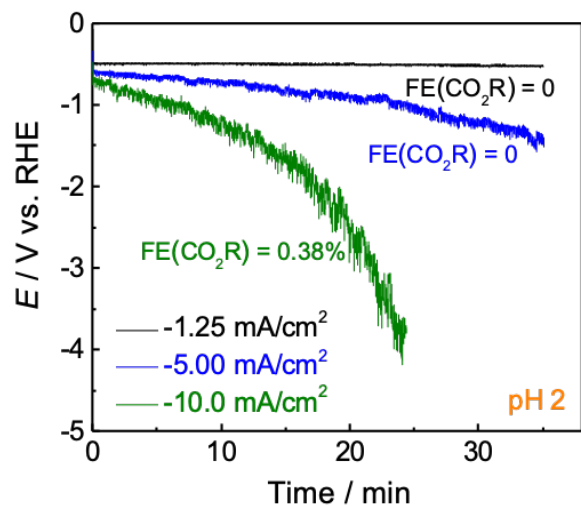


**Figure S3.** The  $E$  profiles with  $FE_{CO_2R}$  on Cu foil electrodes at different  $\langle j \rangle$  in pH 2  $H_3PO_4$ ;

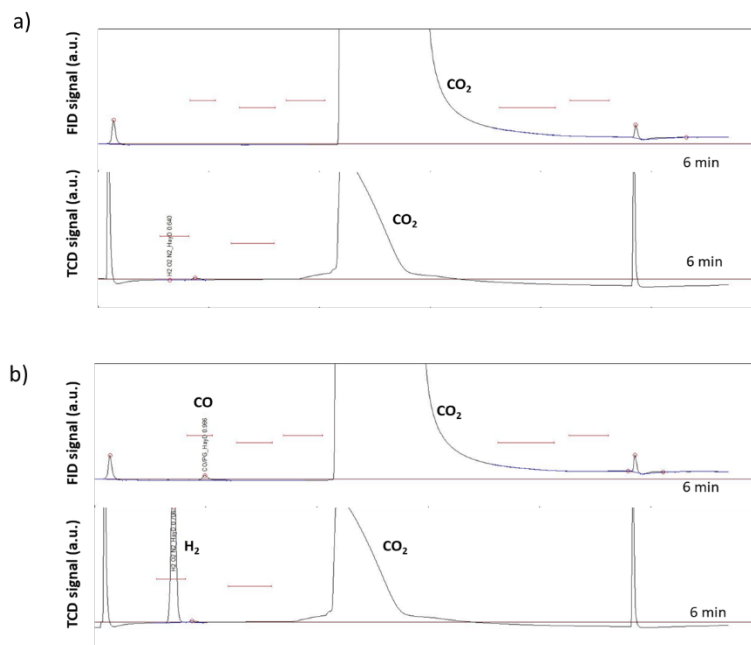


**Figure S4.** Representative GC curves of gas stream from electrolysis at  $-10.0 \text{ mA/cm}^2$  in pH 2  $H_3PO_4$  with 10 mM 18-crown-6 to chelate free  $M^+$  impurity: (a) the background test before electrolysis started; (b) the experimental test after electrolysis started showing  $CO/H_2$  generation.



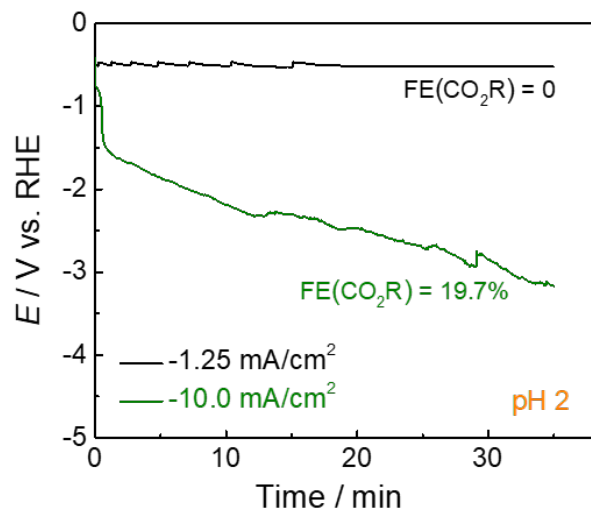


**Figure S5.** (a) The  $E$  profiles of electrolysis on Cu GDE at  $-1.25 \text{ mA/cm}^2$  and  $-10.0 \text{ mA/cm}^2$  in pH 2 and pH 3  $\text{H}_3\text{PO}_4$  and (b) at  $-10.0 \text{ mA/cm}^2$  in pH 2 and pH 1  $\text{H}_3\text{PO}_4$ .

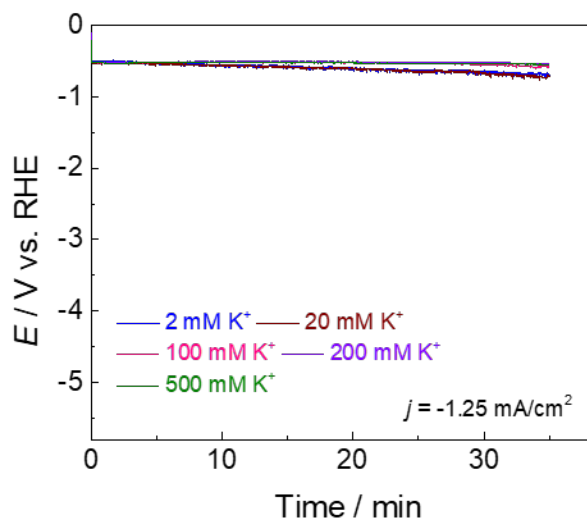


**Figure S6.** The  $E$  profiles of Cu foil electrodes at low  $\langle j \rangle = -1.25 \text{ mA/cm}^2$  in pH 2  $\text{H}_3\text{PO}_4$  with different  $[\text{K}^+]$ .

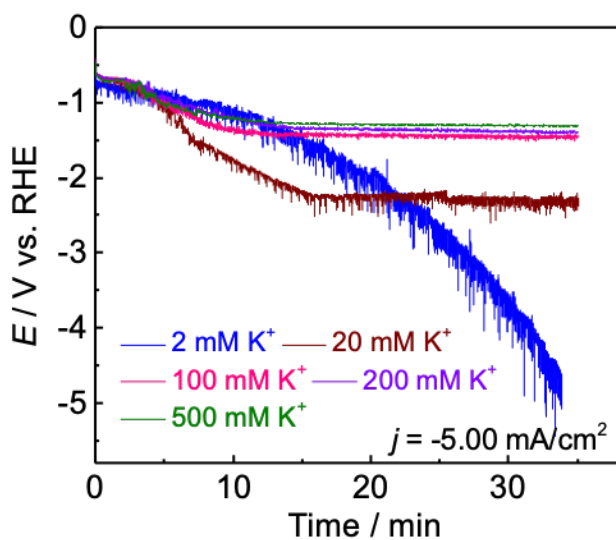


**Figure S7.** The  $E$  profiles of Cu foil electrodes at  $\langle j \rangle = -5.00 \text{ mA/cm}^2$  in pH 2  $\text{H}_3\text{PO}_4$  with different  $[\text{K}^+]$ .

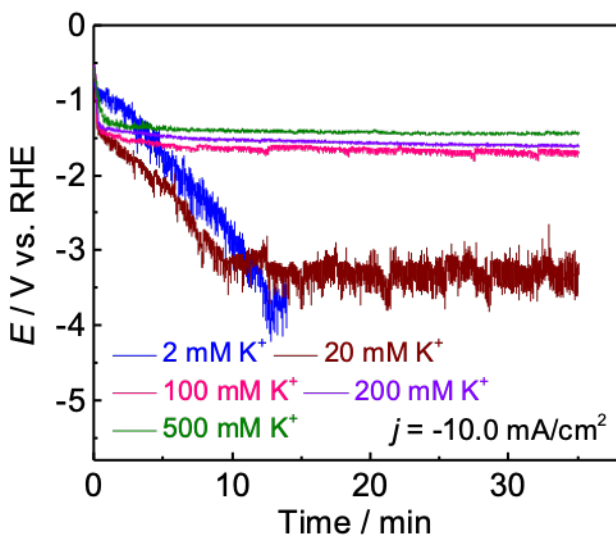


**Figure S8.** The  $E$  profiles of Cu foil electrodes at  $\langle j \rangle = -10.0 \text{ mA/cm}^2$  in pH 2  $\text{H}_3\text{PO}_4$  with different  $[\text{K}^+]$ .

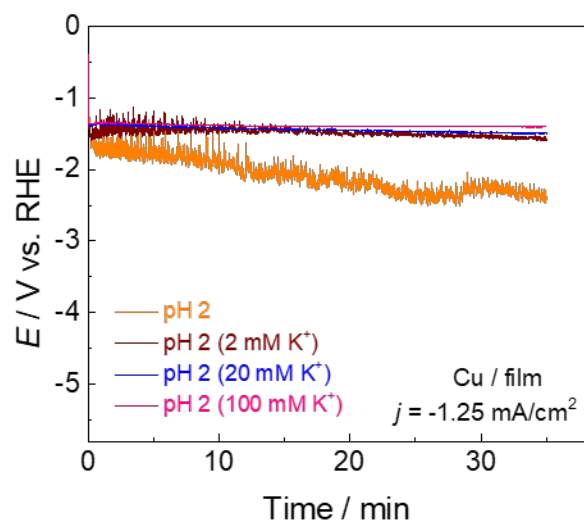


**Figure S9.** The electrode potential  $E$  profiles on modified Cu/film electrodes at low  $-1.25 \text{ mA/cm}^2$  in pH 2  $\text{H}_3\text{PO}_4$  with different  $[\text{K}^+]$ .

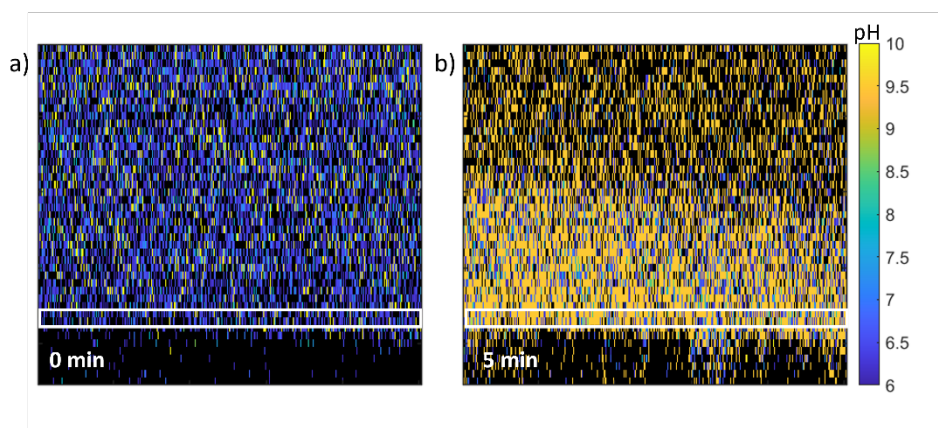


**Figure S10.** Exemplary pH maps in the plane perpendicular to the cathode surface captured with confocal microscopy and the fluorescent dye DHPDS in pH 2  $\text{H}_3\text{PO}_4$  with 20 mM  $\text{K}^+$  at  $-10 \text{ mA/cm}^2$  and 5 SCCM  $\text{CO}_2$  flow at (a) 0 minutes and (b) 5 minutes after starting the current. The white frames indicate the area approximately between the electrode surface and  $1 \mu\text{m}$  above the surface in which the pH value that is displayed in other figures was averaged.

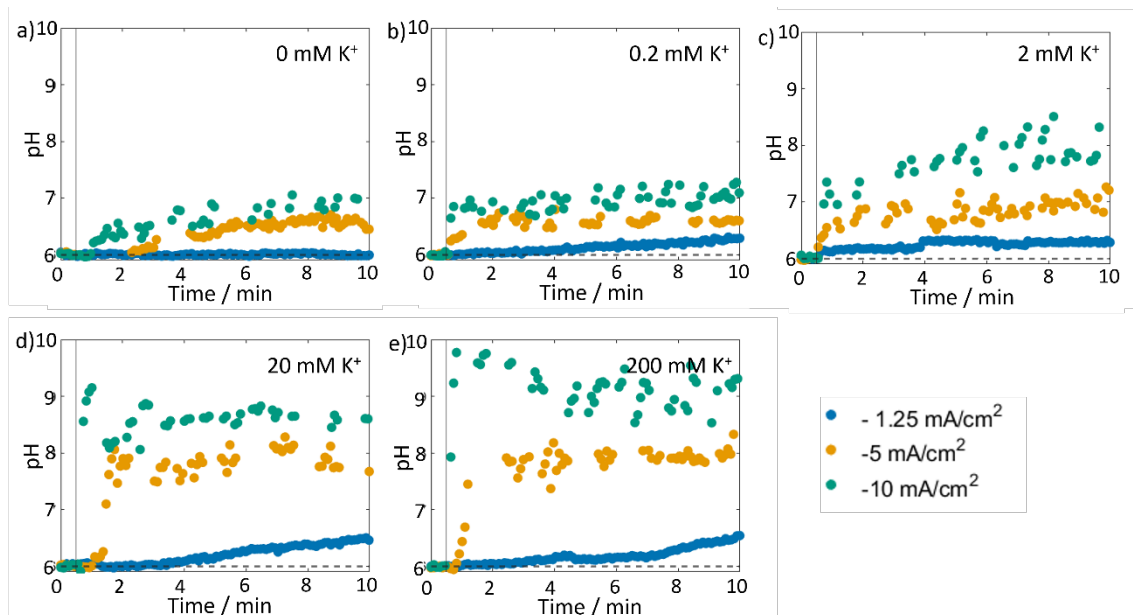


**Figure S11.** Local pH value at the electrode surface as a function of time and current density for (a) 0 mM; (b) 0.2 mM; (c) 2 mM; (d) 20 mM and (e) 200 mM  $[K^+]$  in pH 2  $H_3PO_4$  with 5 SCCM  $CO_2$  flow.

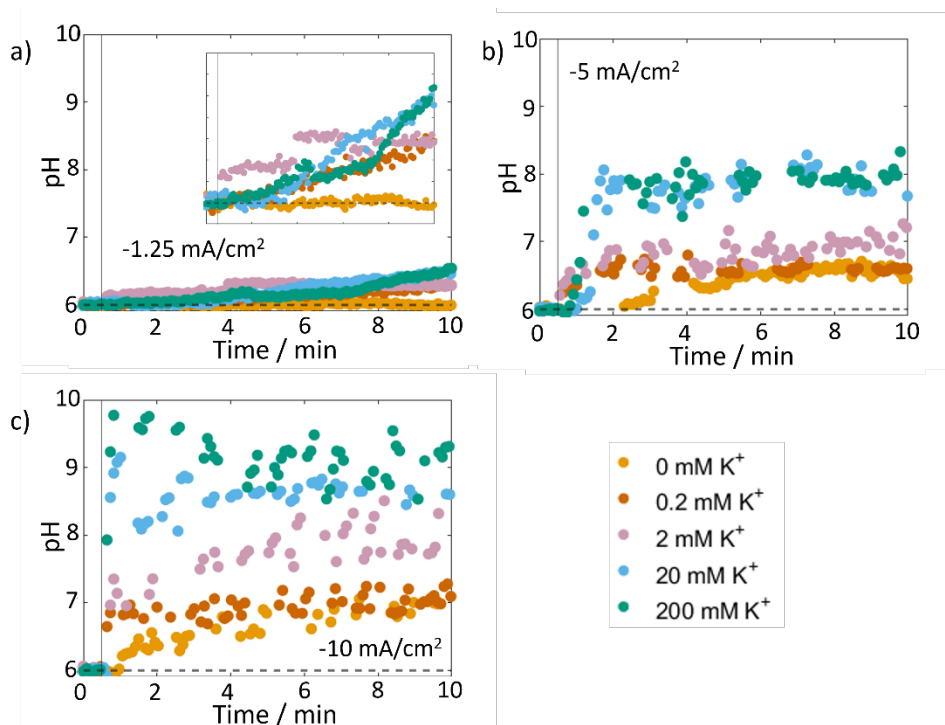


**Figure S12.** Local pH value at the electrode surface as a function of time and  $[K^+]$  for (a)  $-1.25 \text{ mA/cm}^2$  (inset is a zoomed-in version of the same data); (b)  $-5 \text{ mA/cm}^2$  and (c)  $-10 \text{ mA/cm}^2$  in pH 2  $H_3PO_4$  with 5 SCCM  $CO_2$  flow.

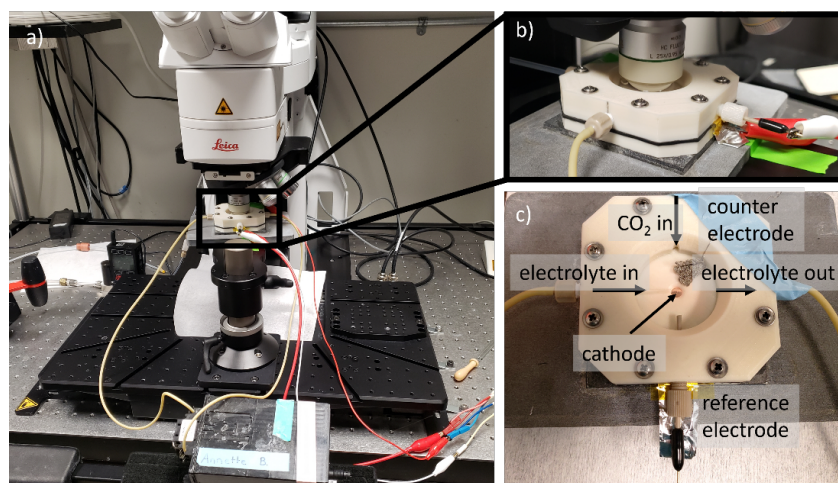


**Figure S13.** Photographs of the CLSM pH imaging setup, (a) Leica Stellaris 5 confocal microscope setup with custom-built electrochemical cell, (b) Close-up of the electrochemical cell and (c) Top-view labelled photograph of the electrochemical cell.

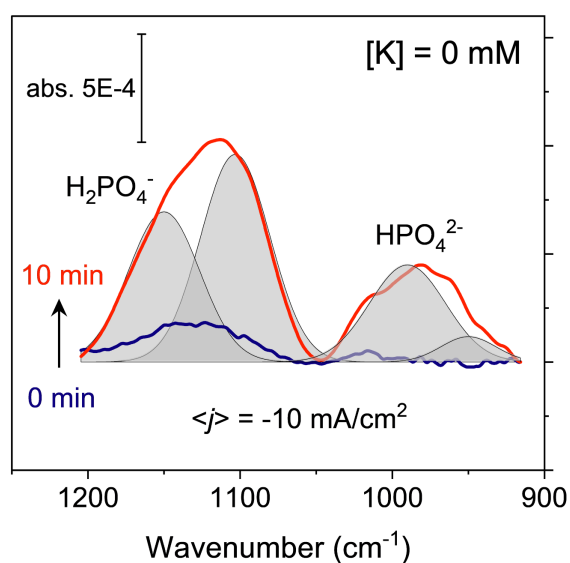


**Figure S14.** SEIRA spectra of the phosphate region with peak deconvolution for 0 mM  $K^+$  in pH 2  $H_3PO_4$  at 0 and 10 minutes of applied  $\langle j \rangle = -10.0 \text{ mA/cm}^2$  demonstrating an increase in interfacial pH evidenced by the rise of the  $HPO_4^{2-}$  band.

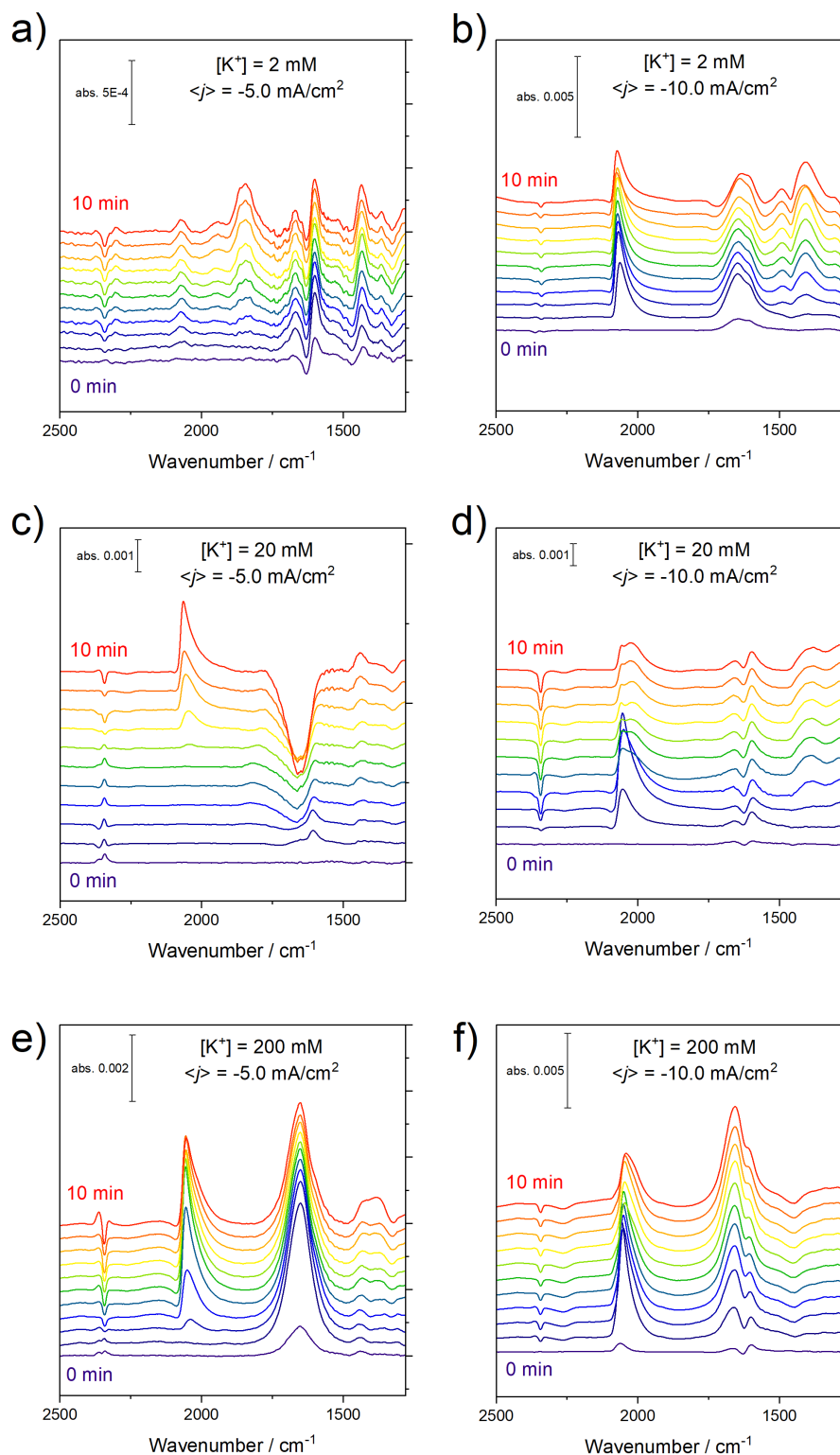


**Figure S15.** Time-dependent SEIRA spectra showing  $CO_2(aq)$ ,  $^*CO$ , H-O-H bending, and (bi)carbonate regions for 2 mM  $K^+$  (a,b); 20 mM  $K^+$  (c,d); 200 mM  $K^+$  (e,f).

**Table S1.** ICP-MS measurement results of pH 2 H<sub>3</sub>PO<sub>4</sub>.

Li <sup>+</sup>	K <sup>+</sup>	Cs <sup>+</sup>	Cu <sup>2+</sup>	Zn <sup>2+</sup>	Ag <sup>+</sup>
0.003 ppm	0.847 ppm	-	2.81 ppb	1.61 ppb	0.029 ppb
$4.3 \times 10^{-4}$ mM	$2.2 \times 10^{-2}$ mM	-	$4.4 \times 10^{-5}$ mM	$2.5 \times 10^{-5}$ mM	$2.7 \times 10^{-7}$ mM

**Table S2.** Faradaic efficiency (FE) towards different products in controlled-current electrolysis on bare Cu foil electrodes in acidic electrolytes at different  $\langle j \rangle$  under CO<sub>2</sub>.

$\langle j \rangle$ / mA·cm <sup>-2</sup>	pH	FE / % <sup>[a]</sup>										
		H <sub>2</sub>	CO	CH <sub>4</sub>	Formate	Acetic acid	C <sub>2</sub> H <sub>4</sub>	Ethanol	1-propanol	C <sub>1</sub>	C <sub>2+</sub>	CO <sub>2</sub> R
-1.25 mA/cm <sup>2</sup>	pH 2	96.9 ±	0	0	0	0	0	0	0	0	0	0
		7.3										
-5.00 mA/cm <sup>2</sup>	pH 2	94.8 ±	0	0	0	0	0	0	0	0	0	0
		2.7										
-10.0 mA/cm <sup>2</sup>	pH 2	92.1 ±	0.1 ±	0.1 ±	0.2 ± 0.2	0	0	0	0	0.4 ±	0	0.4 ±
		2.0	0.04	0.01						0.2		0.2
-1.25 mA/cm <sup>2</sup>	pH 3	100.4 ±	0.7 ±	0	0	0	0	0	0	0.7 ±	0	0.7 ±
		0.8	0.2							0.2		0.2
-10.0 mA/cm <sup>2</sup>	pH 1	96.0 ±	0	0	0	0	0	0	0	0	0	0
		0.4										

[a] Reported values are averages from multiple independent measurements with reported standard deviations.

**Table S3.** Faradaic efficiency (FE) towards different products in controlled-current electrolysis on Cu GDE electrodes in pH 2 H<sub>3</sub>PO<sub>4</sub> at different  $\langle j \rangle$  with 5 sccm CO<sub>2</sub> flow.

$\langle j \rangle$ / mA·cm <sup>-2</sup>	pH	FE / % <sup>[a]</sup>										
		H <sub>2</sub>	CO	CH <sub>4</sub>	Formate	Acetic acid	C <sub>2</sub> H <sub>4</sub>	Ethanol	1-propanol	C <sub>1</sub>	C <sub>2+</sub>	CO <sub>2</sub> R
-1.25 mA/cm <sup>2</sup>	pH 2	102.4 ±	0	0	0	0	0	0	0	0	0	0
		0.7										
-10.00 mA/cm <sup>2</sup>	pH 2	73.4 ±	10.5 ±	0.1 ±	8.9 ± 1.5	0	0.3 ±	0	0	19.4 ±	0.3 ±	19.8 ±
		5.8	3.6	0.04			0.2			5.1	0.2	5.4

[a] Reported values are averages from multiple independent measurements with reported standard deviations.

**Table S4.** the bulk pH of electrolytes after 35 min controlled-current electrolysis on Cu foil electrodes at different  $\langle j \rangle$ .

Electrolyte	pH		
	$-1.25 \text{ mA/cm}^2$	$-5.00 \text{ mA/cm}^2$	$-10.0 \text{ mA/cm}^2$
pH 2	2	2	2
pH 2 0.2 mM $\text{K}^+$	2	2	2
pH 2 2.0 mM $\text{K}^+$	2	2.5	2.5

**Table S5.** Faradaic efficiency (FE) towards different products in electrolysis on Cu foil electrodes in pH 2  $\text{H}_3\text{PO}_4$  with different  $[\text{K}^+]$  under  $\text{CO}_2$  at  $\langle j \rangle = -1.25 \text{ mA/cm}^2, -5.00 \text{ mA/cm}^2$  and  $-10.0 \text{ mA/cm}^2$ .

$[\text{K}^+] / \text{mM}$	FE / % <sup>[a]</sup>										
	$\text{H}_2$	CO	$\text{CH}_4$	Formate	Acetic acid	$\text{C}_2\text{H}_4$	Ethanol	1-propanol	$\text{C}_1$	$\text{C}_{2+}$	$\text{CO}_2\text{R}$
pH 2 / $\langle j \rangle = -1.25 \text{ mA/cm}^2$											
0.2	$100.9 \pm 1.3$	0	0	0	0	0	0	0	0	0	0
2.0	$105.9 \pm 2.1$	0	0	0	0	0	0	0	0	0	0
20	$104.0 \pm 1.5$	0	0	0	0	0	0	0	0	0	0
100	$100.0 \pm 0.9$	0	0	0	0	0	0	0	0	0	0
200	$102.0 \pm 0.5$	0	0	0	0	0	0	0	0	0	0
500	$104.6 \pm 0.03$	0	0	0	0	0	0	0	0	0	0
pH 2 / $\langle j \rangle = -5.00 \text{ mA/cm}^2$											
0.2	$95.5 \pm 0.6$	0	0	0	0	0	0	0	0	0	0
2.0	$85.7 \pm 2.8$	$0.9 \pm 0.1$	$2.7 \pm 1.5$	$3.0 \pm 0.1$	0	$1.5 \pm 0.9$	0	0	$6.6 \pm 1.5$	$1.5 \pm 0.9$	$8.1 \pm 2.4$



20	67.2 ± 9.6	1.8 ± 0.3	6.2 ± 2.1	3.8 ± 0.4	0	7.5 ± 3.5	6.4 ± 1.4	0	11.8 ± 2.1	13.8 ± 4.9	25.7 ± 6.9
100	61.7 ± 0.7	2.4 ± 0.01	7.1 ± 0.7	10.9 ± 0.9	0.8 ± 0.03	5.4 ± 1.1	4.4 ± 1.3	0	20.5 ± 1.6	10.6 ± 1.5	31.0 ± 0.1
200	69.5 ± 4.3	2.7 ± 0.1	5.8 ± 0.6	10.8 ± 1.6	1.5 ± 0.03	3.6 ± 1.0	3.4 ± 0.5	0	19.3 ± 2.2	8.5 ± 1.5	27.8 ± 0.1
500	70.6 ± 1.0	2.5 ± 0.2	6.1 ± 2.3	9.9 ± 0.8	1.0 ± 0.7	3.4 ± 0.6	1.9 ± 1.4	0	18.4 ± 1.4	6.3 ± 1.1	24.8 ± 2.3
pH 2 / <j> = -10.0 mA/cm <sup>2</sup>											
0.2	92.1 ± 0.1	0.1 ± 0.1	0.1 ± 0.07	0.4 ± 0.01	0	0	0	0	0.6 ± 0.2	0	0.6 ± 0.2
2.0	80.8 ± 8.1	0.6 ± 0.1	6.5 ± 3.8	3.0 ± 0.1	0	2.3 ± 1.7	0	0	10.1 ± 3.7	2.3 ± 1.7	12.4 ± 5.4
20	66.5 ± 0.9	0.5 ± 0.1	11.6 ± 1.4	0.5 ± 0.2	0	7.7 ± 0.9	5.3 ± 0.8	1.0 ± 0.9	12.6 ± 1.2	14.0 ± 2.7	26.6 ± 3.9
100	64.6 ± 11.7	0.4 ± 0.1	14.7 ± 2.4	1.8 ± 0.3	0.4 ± 0.3	6.6 ± 5.1	4.2 ± 2.8	1.1 ± 1.1	16.9 ± 2.2	13.7 ± 8.7	29.2 ± 10.9
200	61.7 ± 1.1	0.6 ± 0.3	21.1 ± 0.2	2.9 ± 1.1	1.2 ± 1.1	4.6 ± 0.7	3.0 ± 0.3	0	24.6 ± 1.1	7.6 ± 0.3	33.4 ± 1.4
500	67.7 ± 5.2	0.7 ± 0.2	13.4 ± 1.6	3.3 ± 1.1	1.0 ± 0.1	4.9 ± 2.0	3.1 ± 0.4	0	17.5 ± 2.9	9.0 ± 2.4	26.4 ± 5.3

[a] Reported values are averages from multiple independent measurements with reported standard deviations.

**Table S6.** Faradaic efficiency (FE) towards different products in electrolysis on modified Cu/film electrodes in pH 2 H<sub>3</sub>PO<sub>4</sub> under CO<sub>2</sub> and Ar at -0.50 mA/cm<sup>2</sup>, -1.25 mA/cm<sup>2</sup> and -5.00 mA/cm<sup>2</sup>.

<j>	FE / % <sup>[a]</sup>										
	H <sub>2</sub>	CO	CH <sub>4</sub>	Formate	Acetic acid	C <sub>2</sub> H <sub>4</sub>	Ethanol	1-propanol	C <sub>1</sub>	C <sub>2+</sub>	CO <sub>2</sub> R
Cu/film electrodes / nearly-M <sup>+</sup> -free pH 2											
-0.50 mA/cm <sup>2</sup>	114.6 ± 1.4	2.6 ± 0.3	4.2 ± 0.6	0.6 ± 0.4	0	1.2 ± 0.1	0	0	7.4 ± 1.2	1.2 ± 0.1	8.6 ± 1.1
-1.25 mA/cm <sup>2</sup>	96.8 ± 0.1	1.1 ± 0.2	2.0 ± 0.2	1.7 ± 0.04	0	1.0 ± 0.2	0	0	4.8 ± 0.1	1.0 ± 0.2	5.8 ± 0.1
-5.00 mA/cm <sup>2</sup>	87.5 ± 1.9	0.7 ± 0.1	5.6 ± 2.5	0.6 ± 0.2	0	1.3 ± 0.1	0	0	6.8 ± 2.4	1.3 ± 0.1	8.0 ± 2.3

-1.25 mA/cm <sup>2</sup> under Ar	105.5 ± 0.7	0	0	0	0	0	0	0	0	0	0
--------------------------------------	----------------	---	---	---	---	---	---	---	---	---	---

[a] Reported values are averages from multiple independent measurements with reported standard deviations.

**Table S7.** Faradaic efficiency (FE) towards different products in electrolysis on modified Cu/film electrodes in pH 2 H<sub>3</sub>PO<sub>4</sub> with different [K<sup>+</sup>] under CO<sub>2</sub> at -1.25 mA/cm<sup>2</sup>.

[K <sup>+</sup> ] / mM	FE / % <sup>[a]</sup>										
	H <sub>2</sub>	CO	CH <sub>4</sub>	Formate	Acetic acid	C <sub>2</sub> H <sub>4</sub>	Ethanol	1-propanol	C <sub>1</sub>	C <sub>2+</sub>	CO <sub>2</sub> R
0	96.8 ± 0.1	1.1 ± 0.2	2.0 ± 0.2	1.7 ± 0.04	0	1.0 ± 0.2	0	0	4.8 ± 0.1	1.0 ± 0.2	5.8 ± 0.1
2.0	80.4 ± 4.8	2.2 ± 0.6	0.9 ± 0.04	3.4 ± 0.1	0	9.7 ± 2.8	0	0	6.5 ± 0.7	9.7 ± 2.8	16.2 ± 3.5
20	34.1 ± 6.6	4.1 ± 1.6	3.0 ± 1.3	4.9 ± 2.4	0	27.9 ± 4.8	19.2 ± 3.5	0	12.0 ± 3.8	47.1 ± 7.5	59.2 ± 6.8
100	40.0 ± 4.2	4.9 ± 1.8	4.6 ± 0.3	8.1 ± 4.0	0	25.3 ± 5.6	23.7 ± 3.9	0	17.6 ± 6.1	49.0 ± 9.5	66.6 ± 3.4

[a] Reported values are averages from multiple independent measurements with reported standard deviations.

**Table S8.** Faradaic efficiency (FE) towards different products in electrolysis on Cu-GDE and Cu-GDE/film electrodes in pH 1 H<sub>3</sub>PO<sub>4</sub> with and without 0.1 M K<sup>+</sup> at -50.0 mA/cm<sup>2</sup> with 5 sccm CO<sub>2</sub> flow.

Electrode / Electrolyte	FE / % <sup>[a]</sup>										
	H <sub>2</sub>	CO	CH <sub>4</sub>	Formate	Acetic acid	C <sub>2</sub> H <sub>4</sub>	Ethanol	1-propanol	C <sub>1</sub>	C <sub>2+</sub>	CO <sub>2</sub> R
Cu-GDE pH 1/ 0.1 M K <sup>+</sup>	88.0 ± 3.0	0.004 ± 0.001	0	0	0	0	0	0	0.004 ± 0.001	0	0.004 ± 0.001
Cu-GDE / film pH 1	88.8 ± 0.2	0.03 ± 0.0	0.2 ± 0.01	0	0	0	0	0	0.2 ± 0.01	0	0.2 ± 0.01
Cu-GDE / film pH 1/ 0.1 M K <sup>+</sup>	17.5 ± 2.4	1.1 ± 0.3	2.3 ± 0.6	3.3 ± 0.5	1.3 ± 0.1	24.4 ± 1.1	24.4 ± 1.1	2.8 ± 0.4	6.7 ± 1.4	54.5 ± 5.1	62.5 ± 6.5

[a] Reported values are averages from multiple independent measurements with reported standard deviations.

## References

1. Han, Z.; Kortlever, R.; Chen, H.-Y.; Peters, J. C.; Agapie, T. "CO<sub>2</sub> Reduction Selective for C<sub>2</sub> Products on Polycrystalline Copper with N-Substituted Pyridinium Additives," *ACS Cent. Sci.* **2017**, *3*, 853-859. <http://dx.doi.org/10.1021/acscentsci.7b00180>
2. Lobaccaro, P.; Singh, M. R.; Clark, E. L.; Kwon, Y.; Bell, A. T.; Ager, J. W. "Effects of temperature and gas–liquid mass transfer on the operation of small electrochemical cells for the quantitative evaluation of CO<sub>2</sub> reduction electrocatalysts," *Phys. Chem. Chem. Phys.* **2016**, *18*, 26777-26785. <http://dx.doi.org/10.1039/C6CP05287H>
3. Nie, W.; Heim, G. P.; Watkins, N. B.; Agapie, T.; Peters, J. C. "Organic Additive-derived Films on Cu Electrodes Promote Electrochemical CO<sub>2</sub> Reduction to C<sub>2+</sub> Products Under Strongly Acidic Conditions," *Angew. Chem. Int. Ed.* **2023**, *62*, e202216102. <http://dx.doi.org/https://doi.org/10.1002/anie.202216102>
4. Miyake, H.; Ye, S.; Osawa, M. Electroless Deposition of Gold Thin Films on Silicon for Surface-Enhanced Infrared Spectroelectrochemistry. *Electrochem. Commun.* **2002**, *4* (12), 973–977. [https://doi.org/10.1016/S1388-2481\(02\)00510-6](https://doi.org/10.1016/S1388-2481(02)00510-6).